
What shapes galaxy SEDs?

What shapes galaxy SEDs?

- Stars
- Dust
- Gas

- Key papers
  - Kennicutt 1998; Worthey 1994; Bell & de Jong 2001; Condon 1992; Bell 2003; Calzetti 2001
  - Osterbrock's book…

1/2-2/3 of all energy comes out in IR

Both optical and IR have Combination of

~black body
+
narrower features

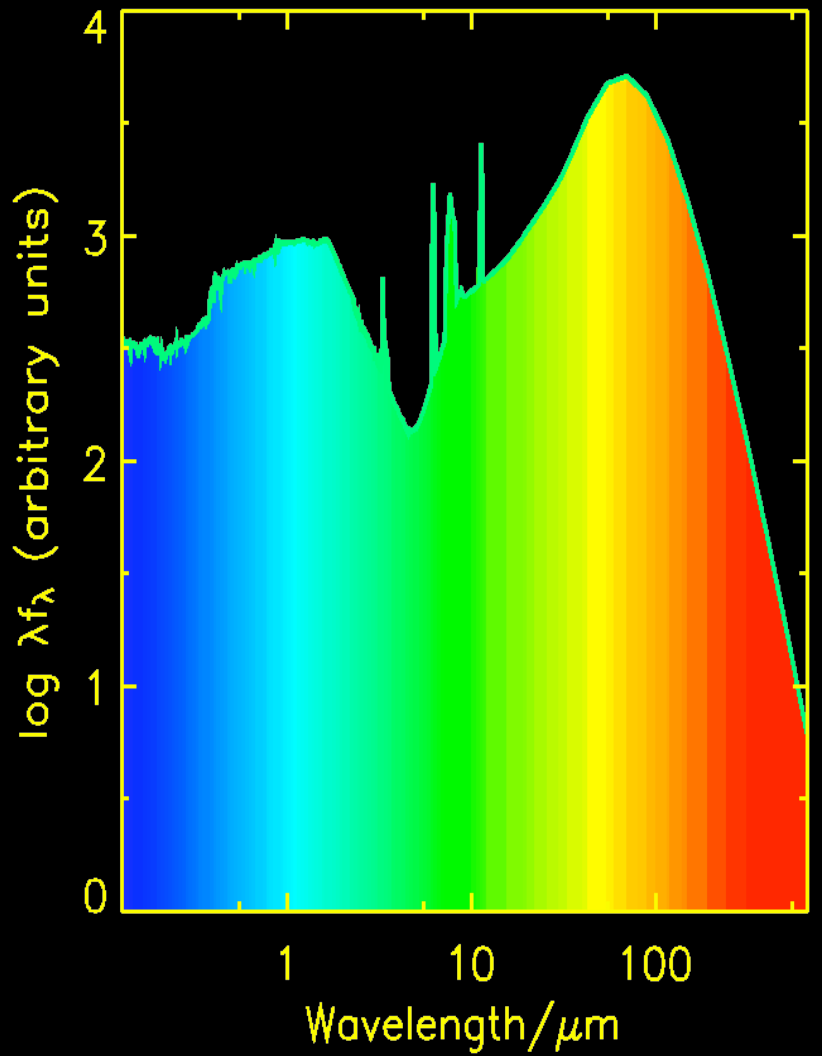

Heidelberg
March-April 2008

Eric Bell

Stars

- Stellar mass-temperature-luminosity-lifetime relation
  - High mass short lived & luminous
  - Low-mass long lived & lower-luminosity

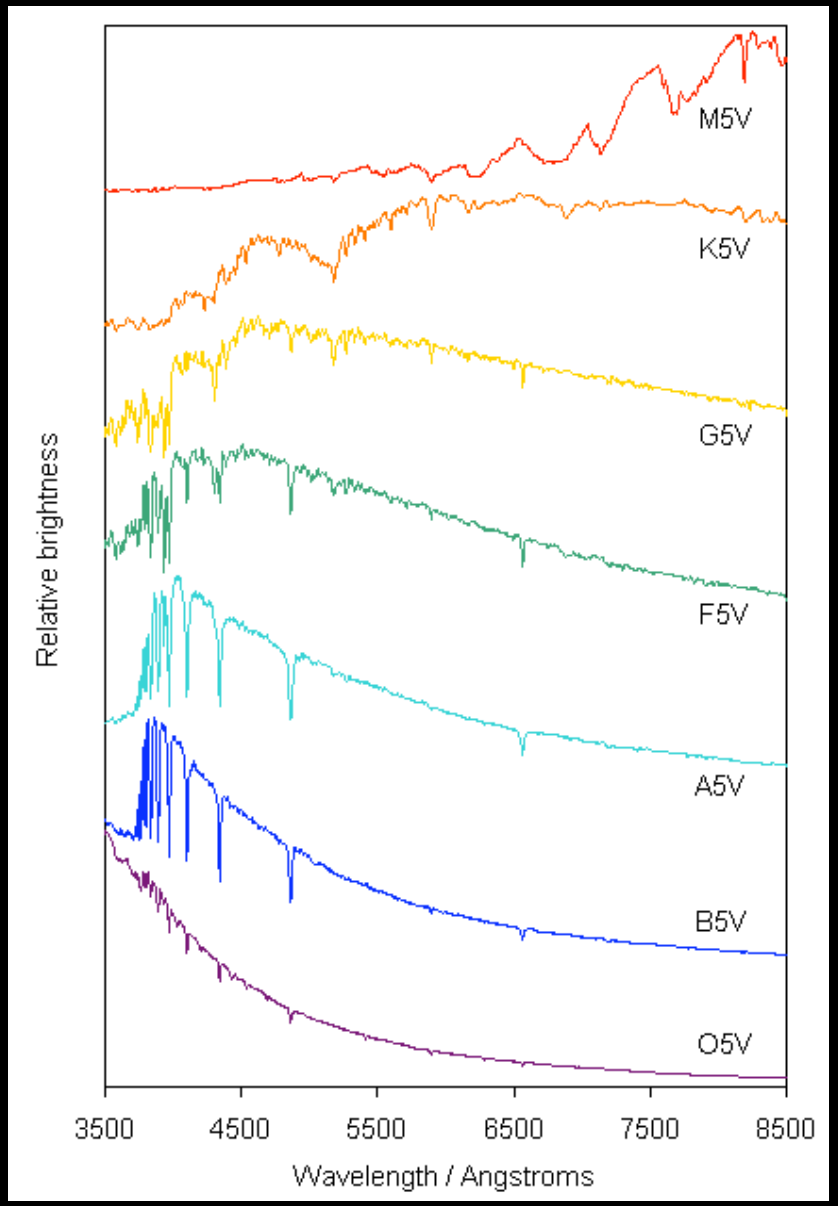

Mix of stellar spectra

- Flux = double integral
  - Star formation /chemical enrichment history (getting from single stellar populations with ages and metallicities to the composite SED)
  - Over stellar initial mass function
    - From stellar spectra --> stellar population spectrum
    - N dm ∝f(m)
    - ($m^{-2.35}$ Salpeter IMF)

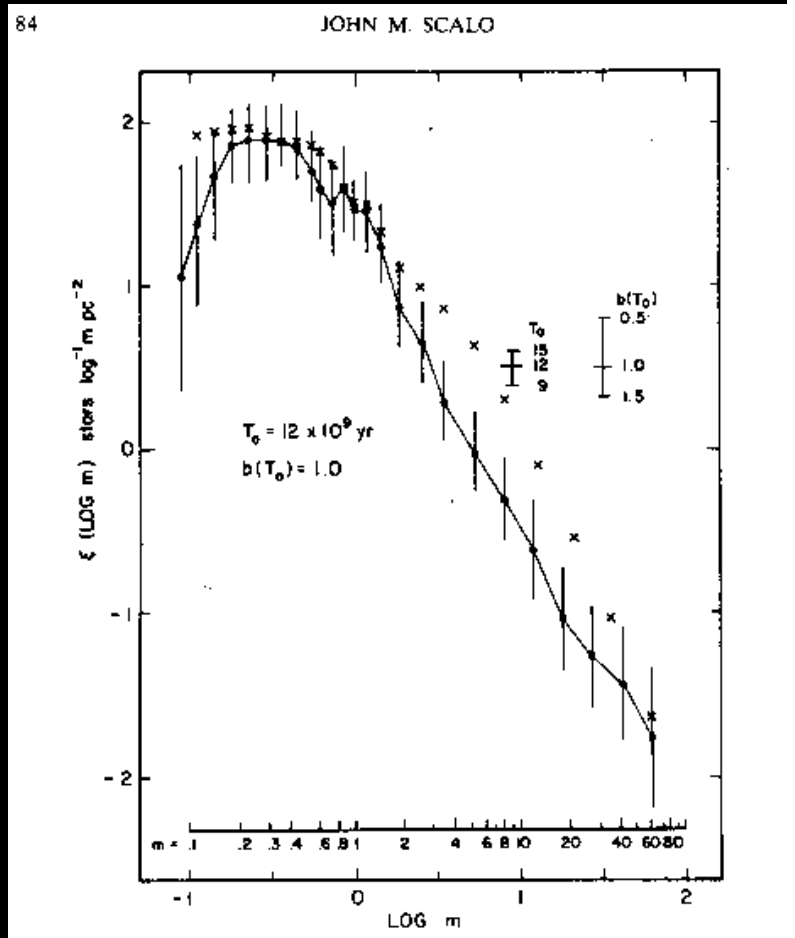

FIGURE 16. Derived field star IMF. Uncertainty estimates do not include relative birthrate $b(T_0)$ and disk age T_0, whose effects are indicated in the figure. Crosses represent the IMF derived in Miller and Scalo (1979).

Heidelberg
March-April 2008

Eric Bell

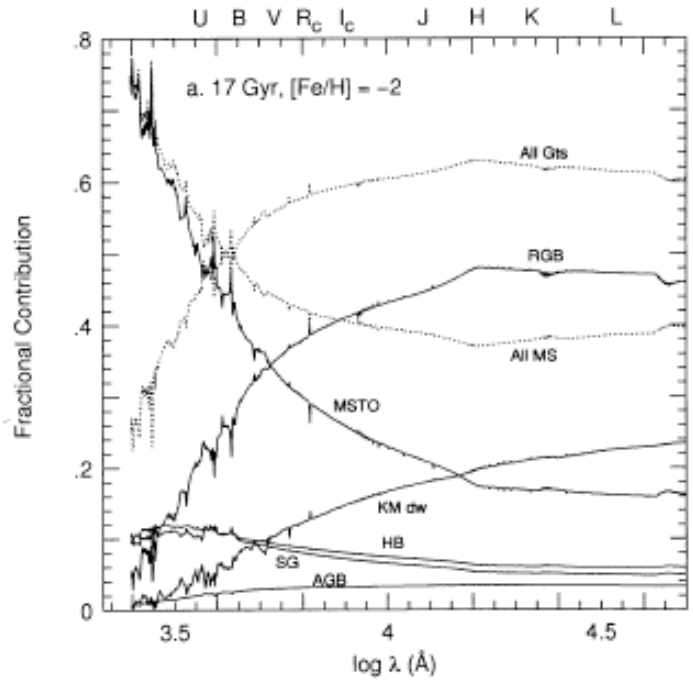

FIG. 41*a*

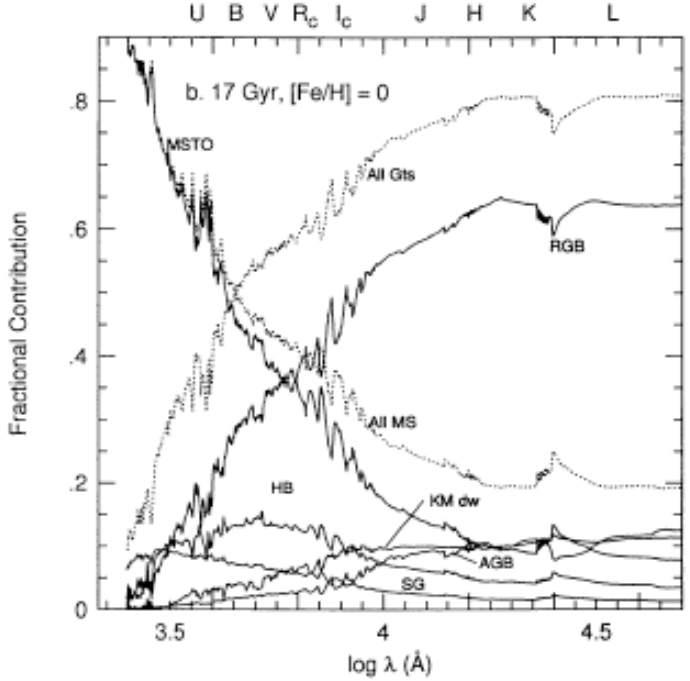

FIG. 41*b*

Worthey et al. 1994

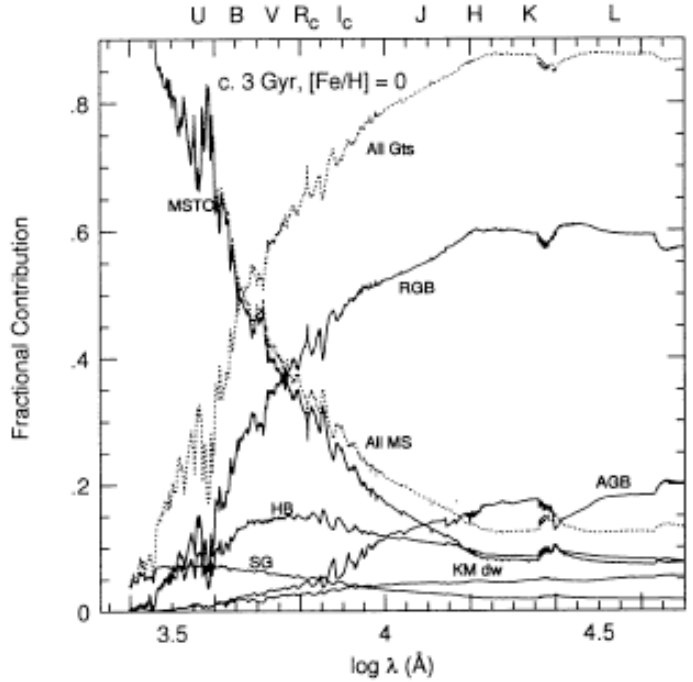

can reasonably expect the models to fit. Fitting function errors or wavelength-dependent errors ought to show up in these diagrams if they are present.

Looking through the diagrams, one sees that the Fe4383 (Fig. 49) index shows no significant offset from the models. There is a fair amount of breadth to the model sequence because young populations have weak Fe4383. Notice that in most of these diagrams M31 lies close to the [Fe/H] = +0.25, age = 8 or 12 Gyr symbols. Ca4455 (Fig. 50) is also in agreement with the models, as is Fe4531 (Fig. 51). Although many galaxies are scattered away from the main locus owing to the presence of nebular emission in the blue pseudocontinuum of the Fe5015 index (Fig. 52), the median locus is well traced by the models. Recall that the galaxy sample is heterogeneous, and emission effects have not been corrected. Fe5335 (Fig. 53) is well matched by the models, but Fe5406 (Fig. 54) suffers from a problem with nebular emission like that of Fe5015. Most galaxies in the Fe5709 plot (Fig. 55) land on the model locus, but M31 does not by several σ. Although it is tempting to speculate on possible causes for such a significant deviation,

Distinctive / important features

- 4000 angstrom break
- 1.6um bump (from a minimum in H- opacity; much of the opacity from stars is from H-)…
- Most important absorption lines
  - Balmer lines, metal lines

Sawicki 2002

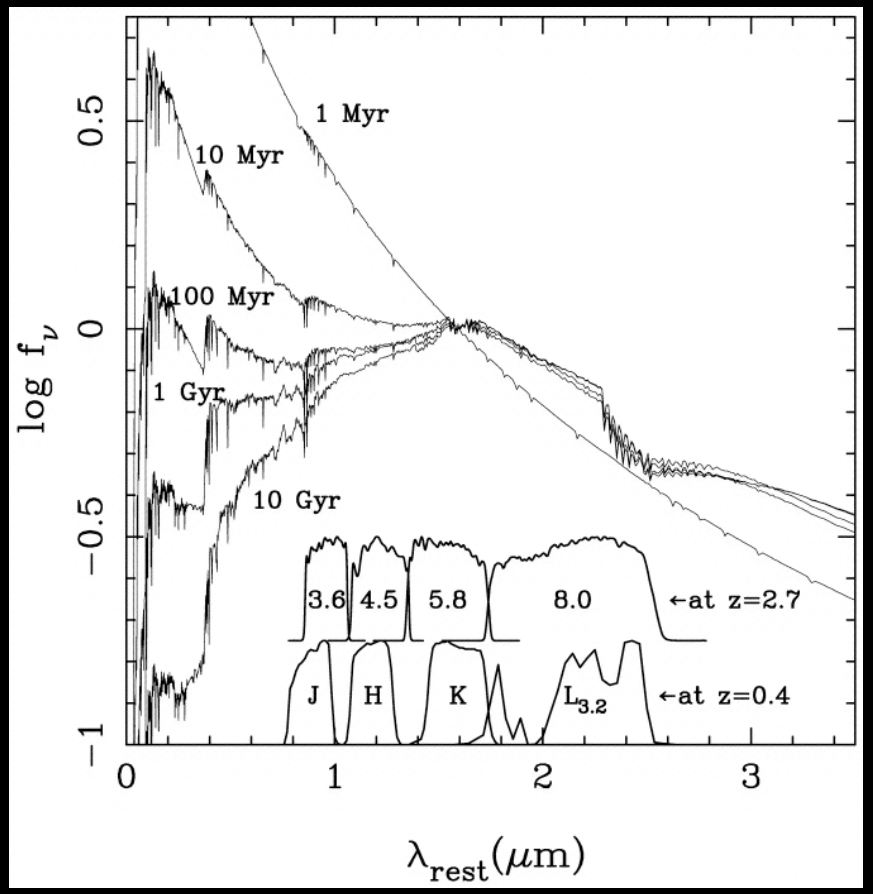

Dust - key concepts

- Absorption of UV/optical photons (1/2 to 2/3 of all energy absorbed + re-emitted)
- Grains re-emit energy

- Grain size distribution
  - PAHs - various benzene-style modes (very small, big molecules, band struc)
  - Very small grains - transient heating
  - Larger grains - eqm heating

Spectrum

Stolen from a talk by Brent Groves

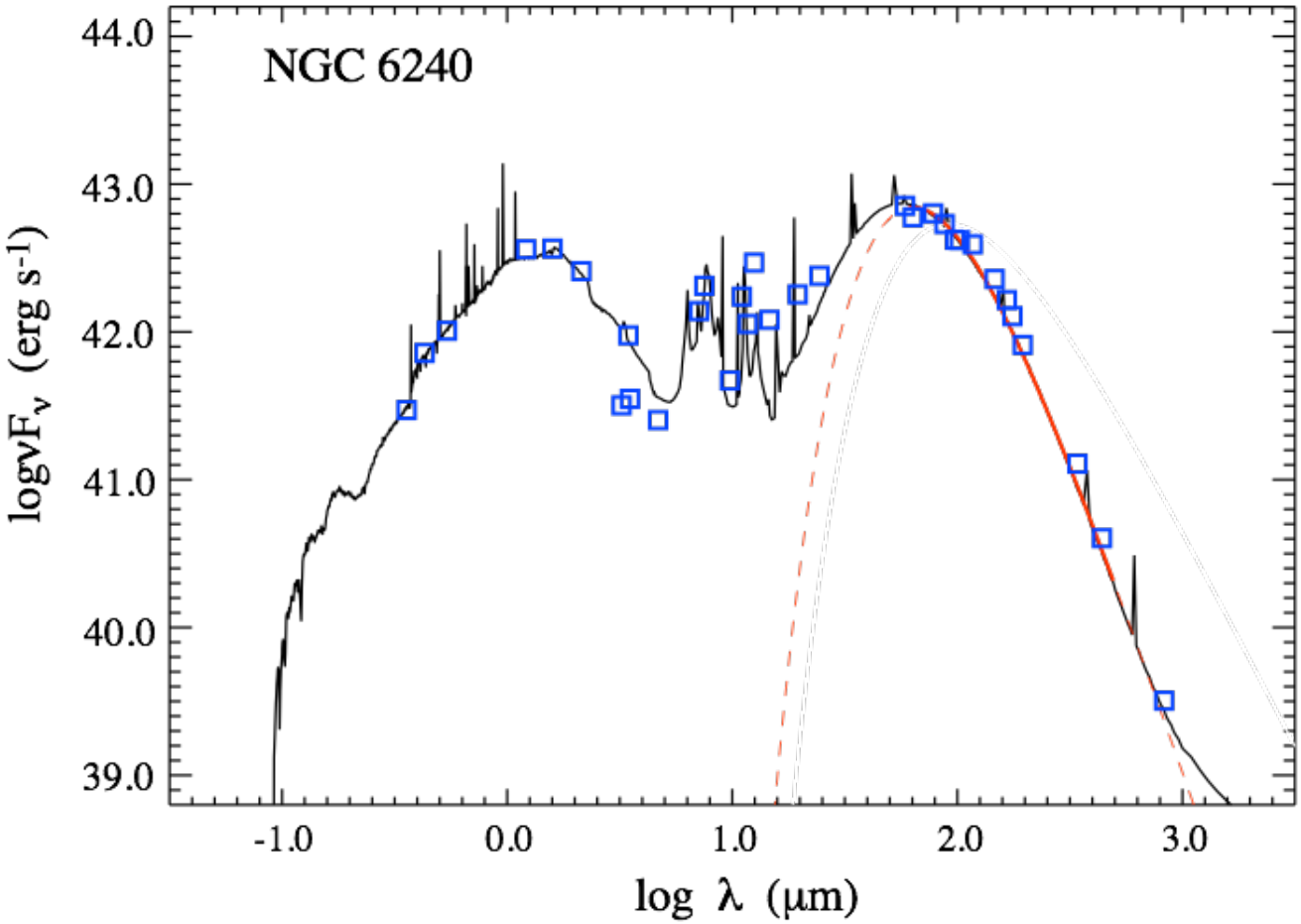

Heidelberg
March-April 2008

Eric Bell

Extinction

- Absorption and scattering
  - Thus, geometry is critical
- Optically-thick distributions behave less intuitively

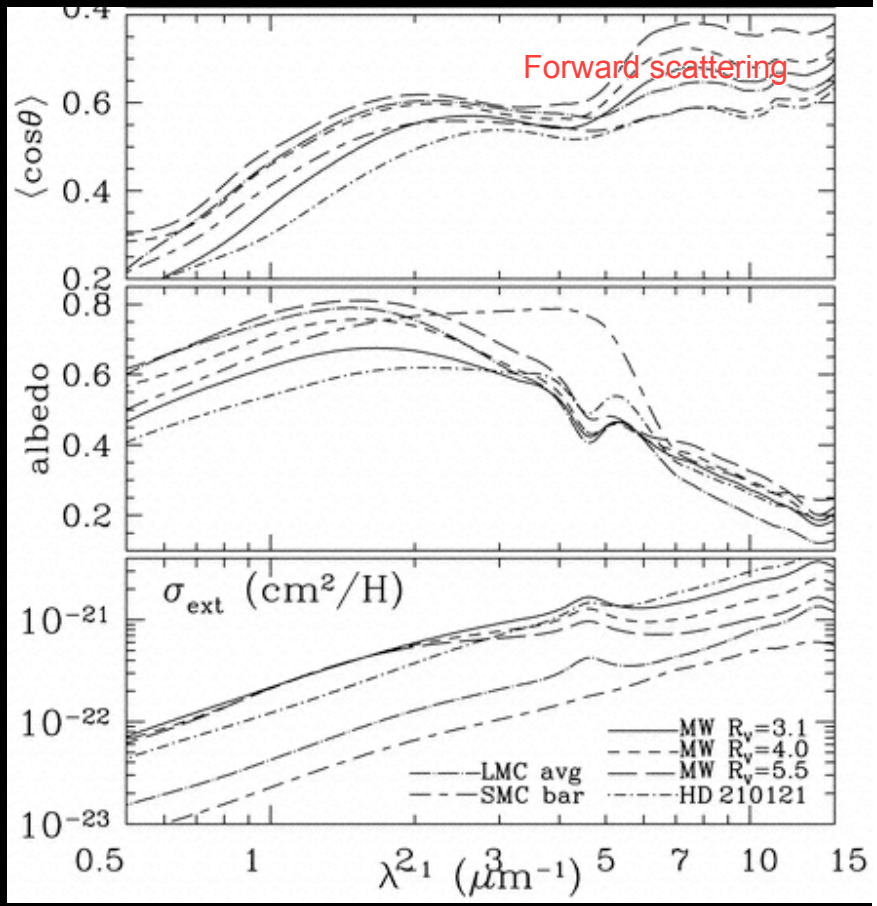

Draine 2003

Extinction

- Extinction curve is variable, esp in FUV
  - Argues shocks / radiation field from nearby star formation - Gordon et al. 2003

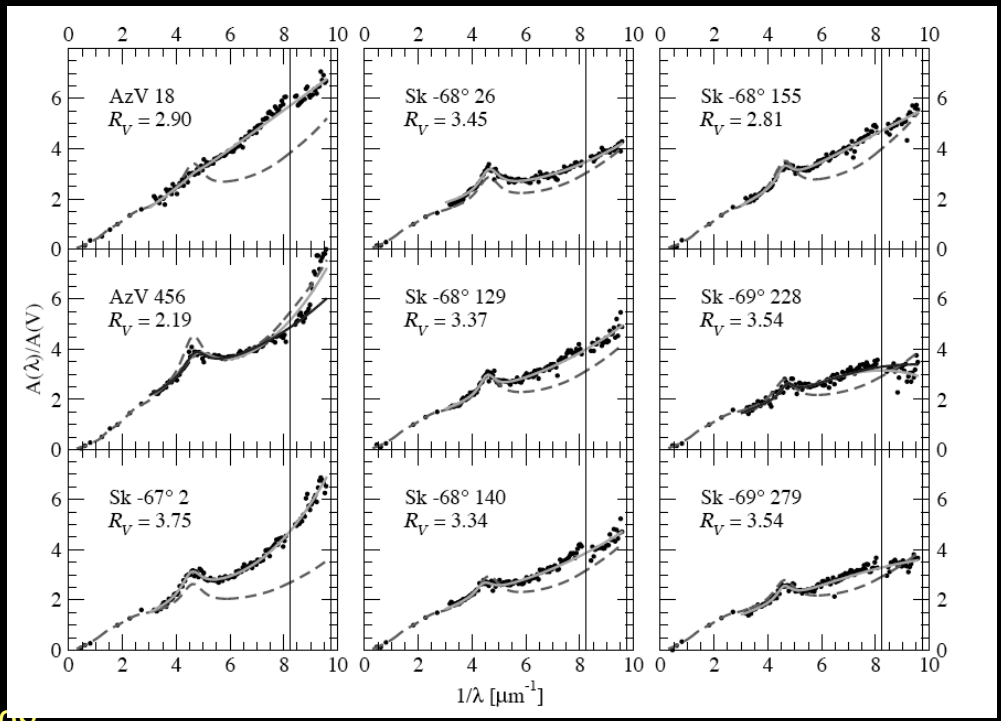

Cartledge et al. 2005

Attenuation vs. extinction

- Excinction curve = for a star, absorption and scattering
- Attenuation curve = for a galaxy, a complicated mix of absorption, scattering and geometry
  - See e.g., Witt & Gordon 2000 for a discussion…

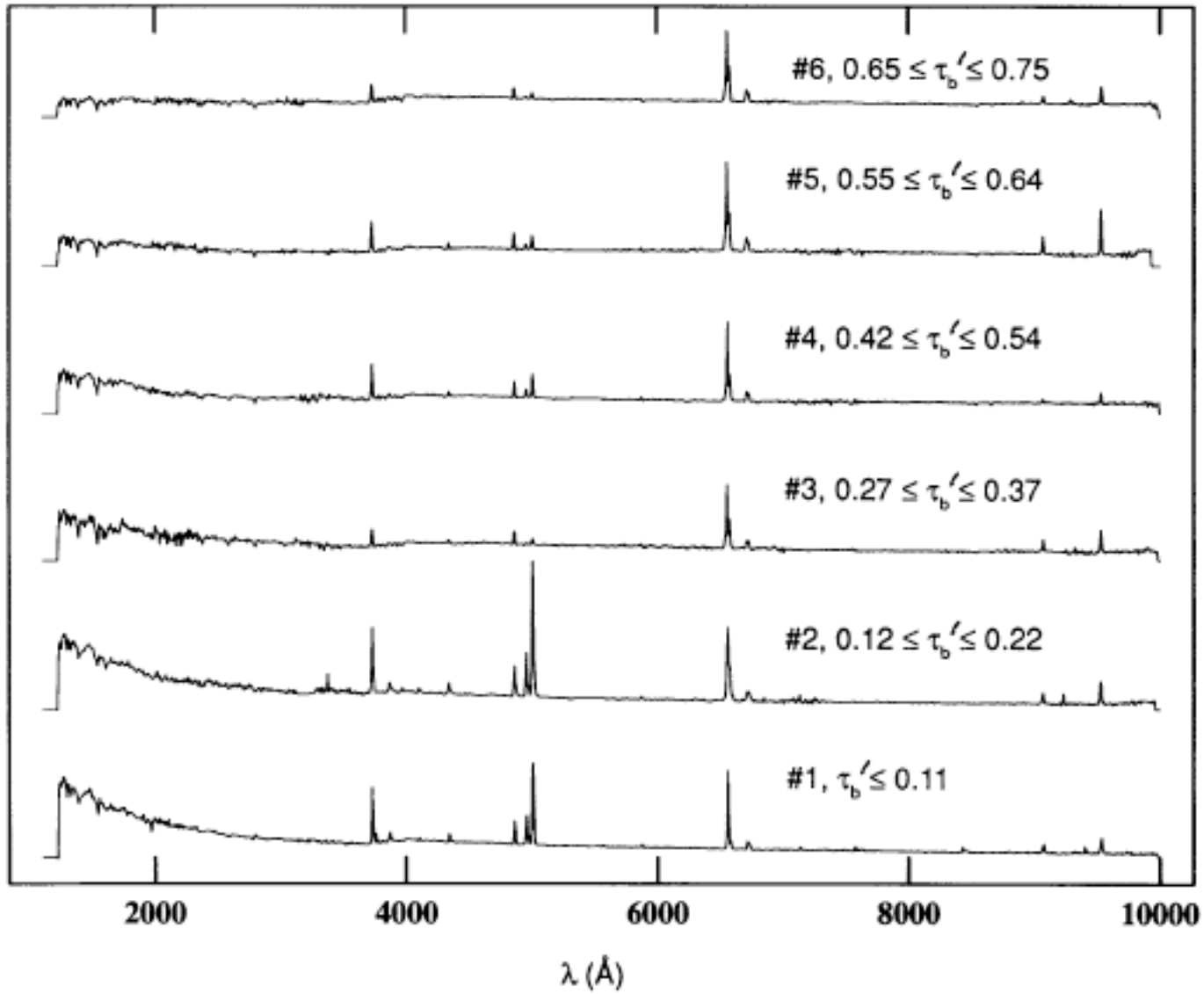

FIG. 17.—The spectra of the six templates are shown for increasing values of the extinction parameter τ_B^l, from the bottom to the top of the figure.

ng,

(7)

(8a)

for $0.12\ \mu\text{m} \leq \lambda < 0.63\ \mu\text{m}$. (8b)

Simple toy model consideration

- Optical depth ∝ gas surface density * metallicity
  - Motivation - dust/gas ∝ metallicity
  - Total dust column ∝ gas column

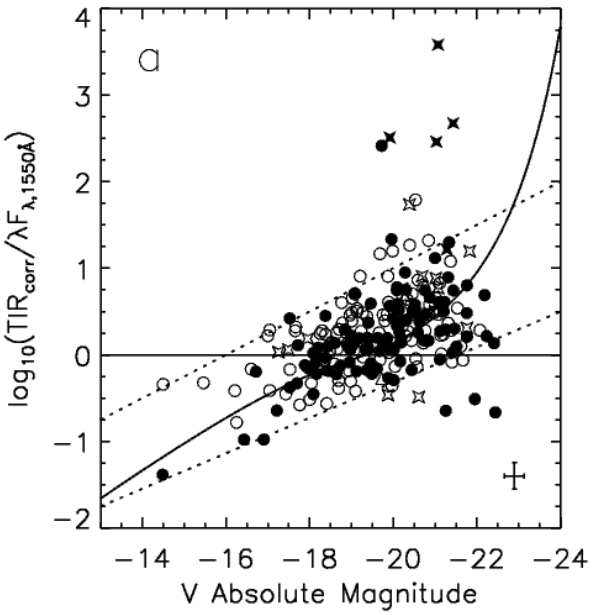

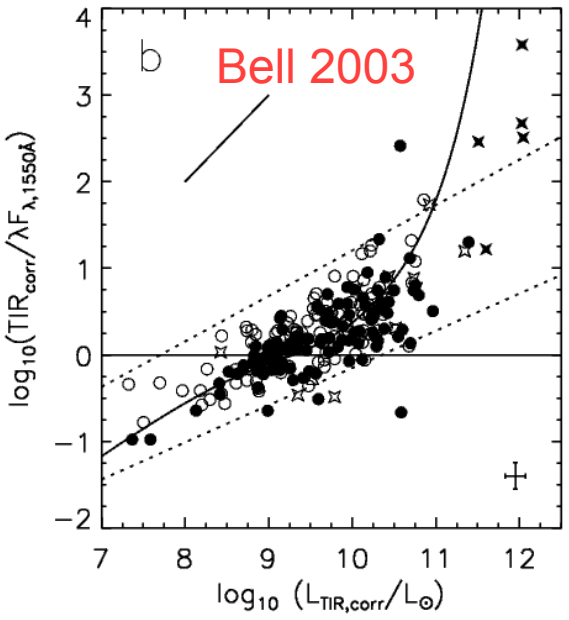

Eric Bell

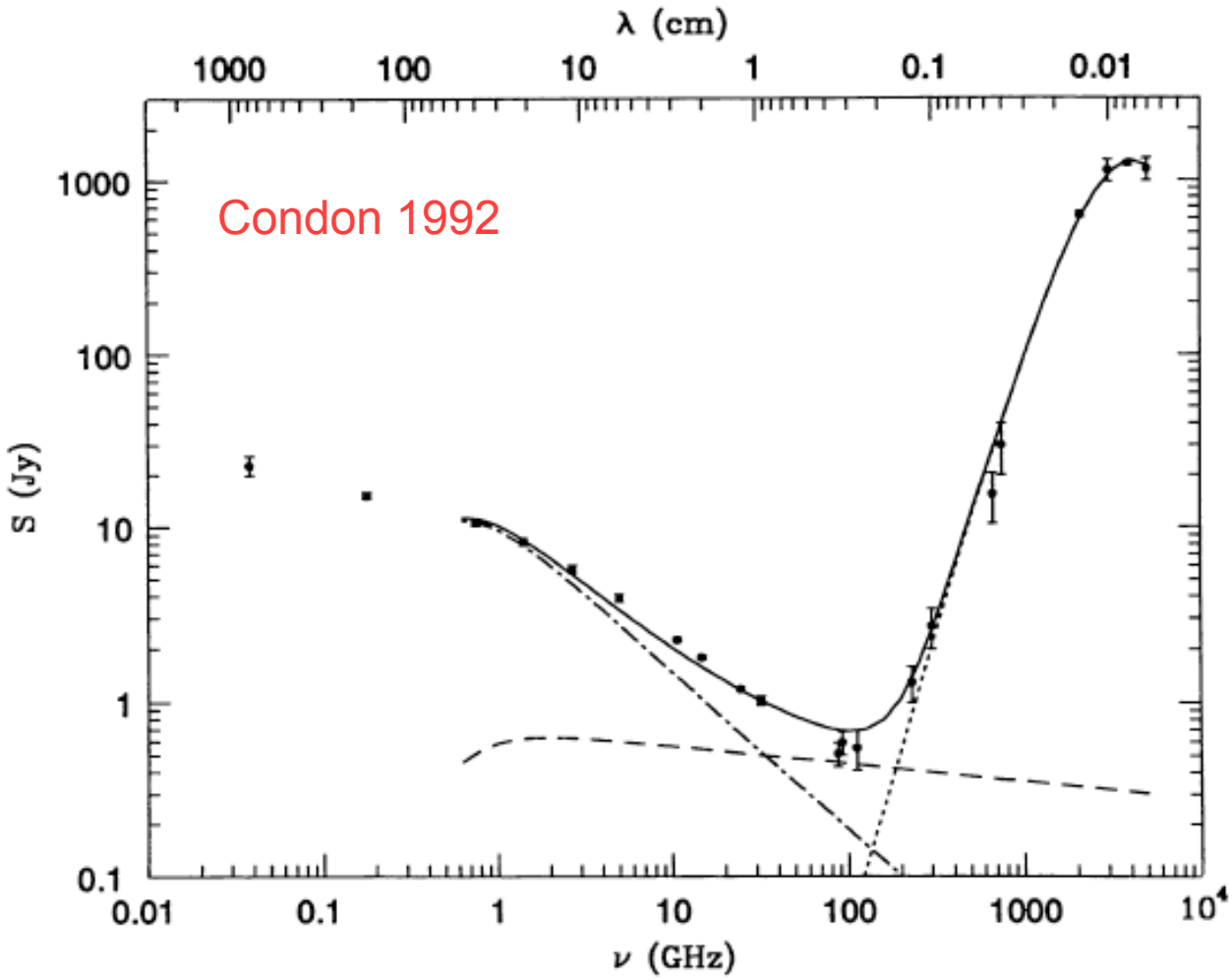

Figure 1 The observed radio/FIR spectrum of M82 (Klein et al 1988, Carlstrom & Kronberg 1991) is the sum (*solid line*) of synchrotron (*dot-dash line*), free-free (*dashed line*), and dust (*dotted line*) components. The H II regions in this bright starburst galaxy start to become opaque below $\nu \sim 1$ GHz, reducing both the free-free and synchrotron flux densities. The free-free component is largest only in the poorly observed frequency range 30–200 GHz. Thermal reradiation from $T \sim 45$ K dust with opacity proportional to $\nu^{1.5}$ swamps the radio emission at higher frequencies. Lower abscissa: frequency (GHz). Upper abscissa: wavelength (cm). Ordinate: flux density (Jy).

Emission lines

- Ionised gas
  - Low-energy lines (<few keV) from SF
  - Higher-excitation lines (>10 keV) collisions and AGN

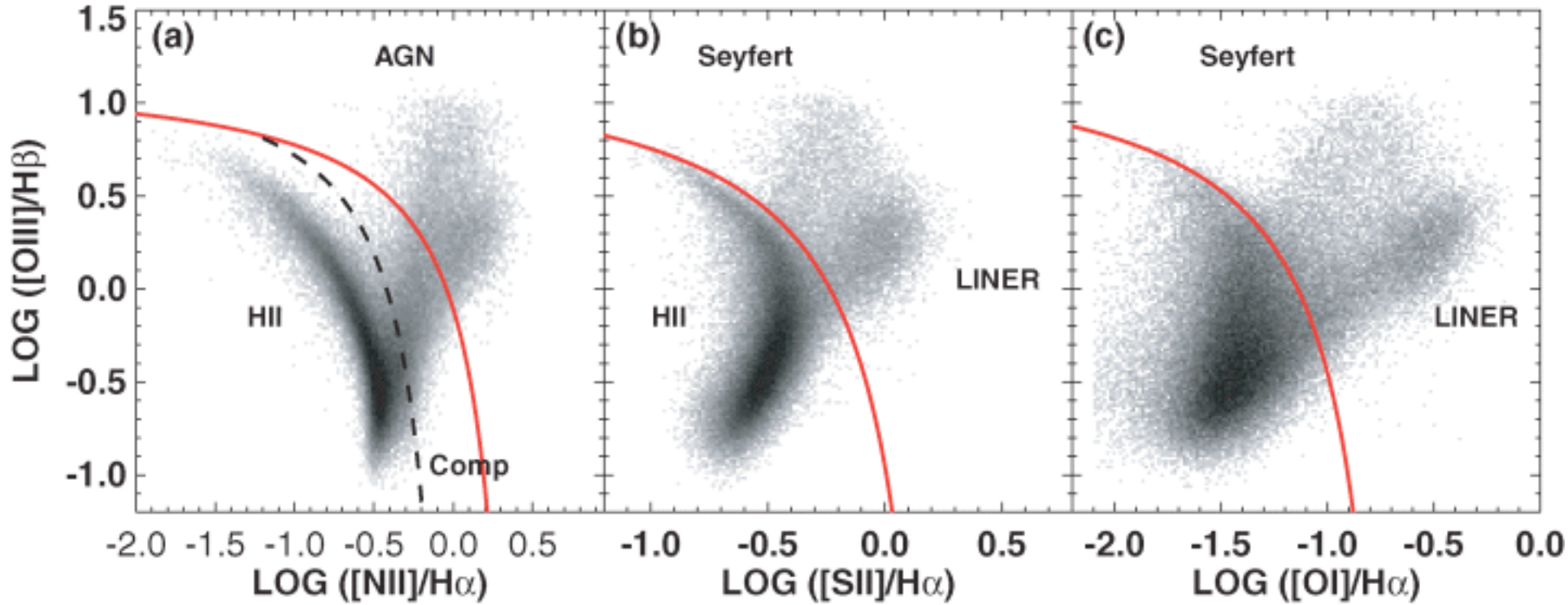

Kewley et al. 2006

Summary...

Near-infrared
dominated by
long-lived stars

Ultraviolet
direct light from young stars

Thermal infrared
dust-reprocessed light
from young stars

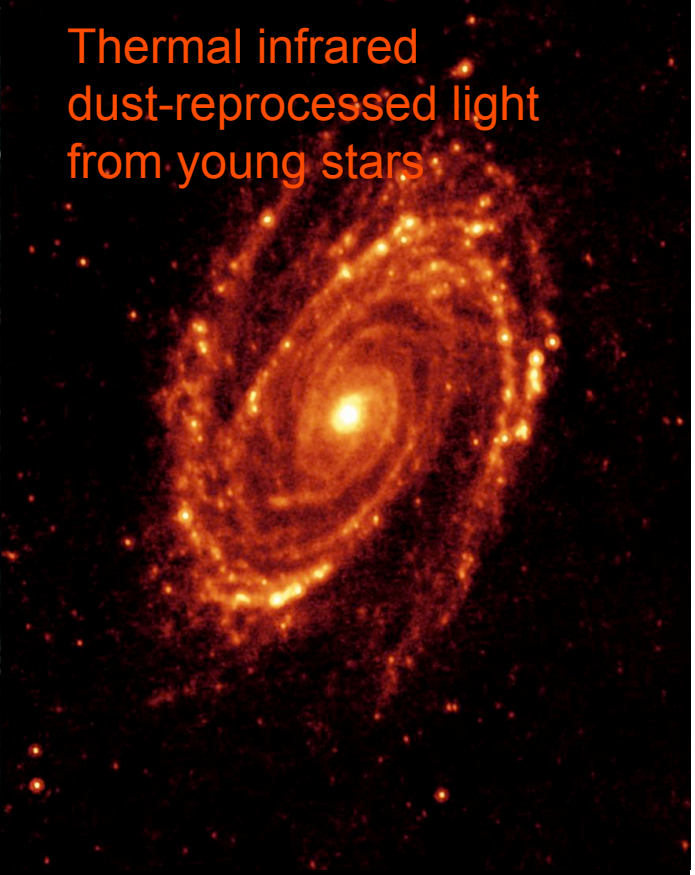

Heidelberg
March-April 2008

Eric Bell

The goal

- Transform observables
  - Spectrum (spatial resolved, wavelength coverage)
  - Into physical parameters
- Horribly ill-posed inversion problem
- Must make critical assumptions
  - This is where the art of the field is…

Interpretation of spectra ar

- C
  -
  -

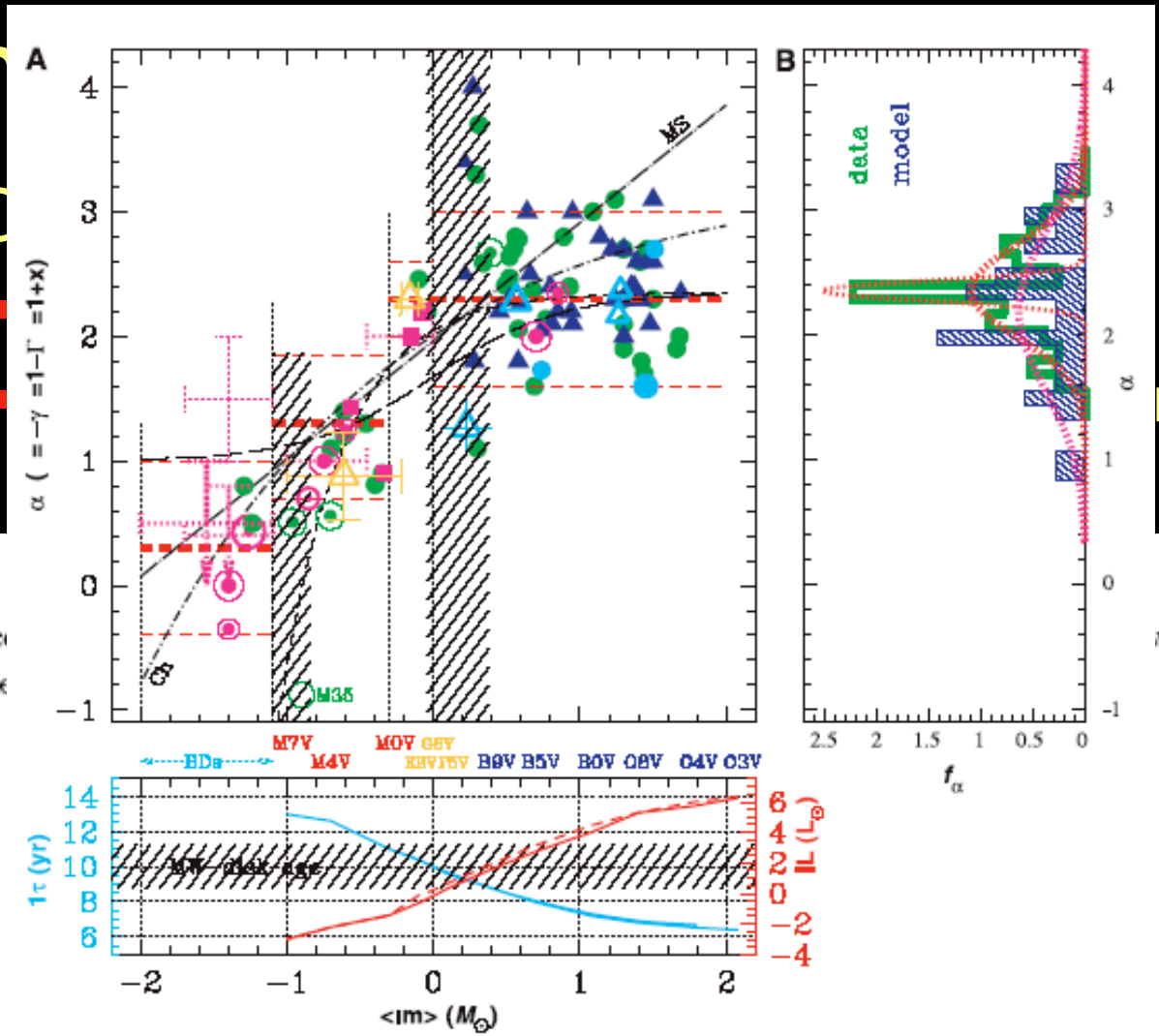

The available c … r IMF (see Kroupa 2001b for de …

(1)

where

(2)

and $\xi(m)\,dm$ is the number of single stars in the mass interval m to $m + dm$. The uncertainties correspond approximately to 99 per cent confidence intervals for $m \gtrsim 0.5\,M_\odot$ (Fig. 1), and to a 95 per cent confidence interval for $0.1 - 0.5\,M_\odot$ (KTG93). Below $0.08\,M_\odot$ the confidence range is not well determined.

Colors

- Age / metallicity / dust degeneracy
- Wide wavelength range starts to help break degeneracies…
  - Ongoing SF vs. metallicity/age

Bell et al. 2003

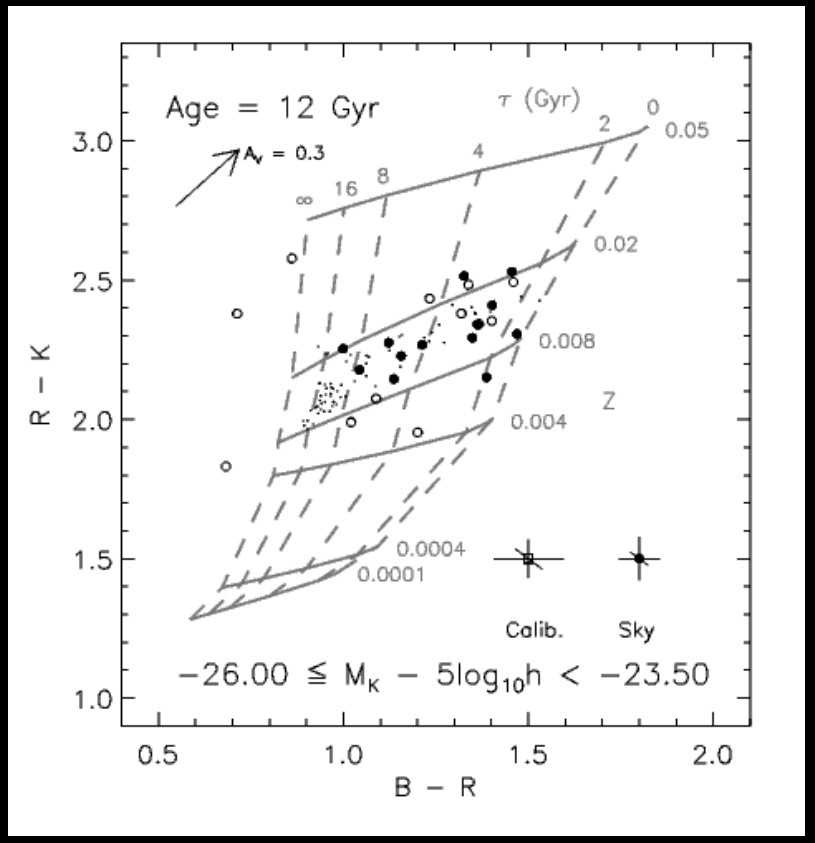

Heidelberg
March-April 2008

The challenges

- **The age-metallicity degeneracy:**
  - *Young, metal-rich populations strongly resemble old, metal-poor populations.*

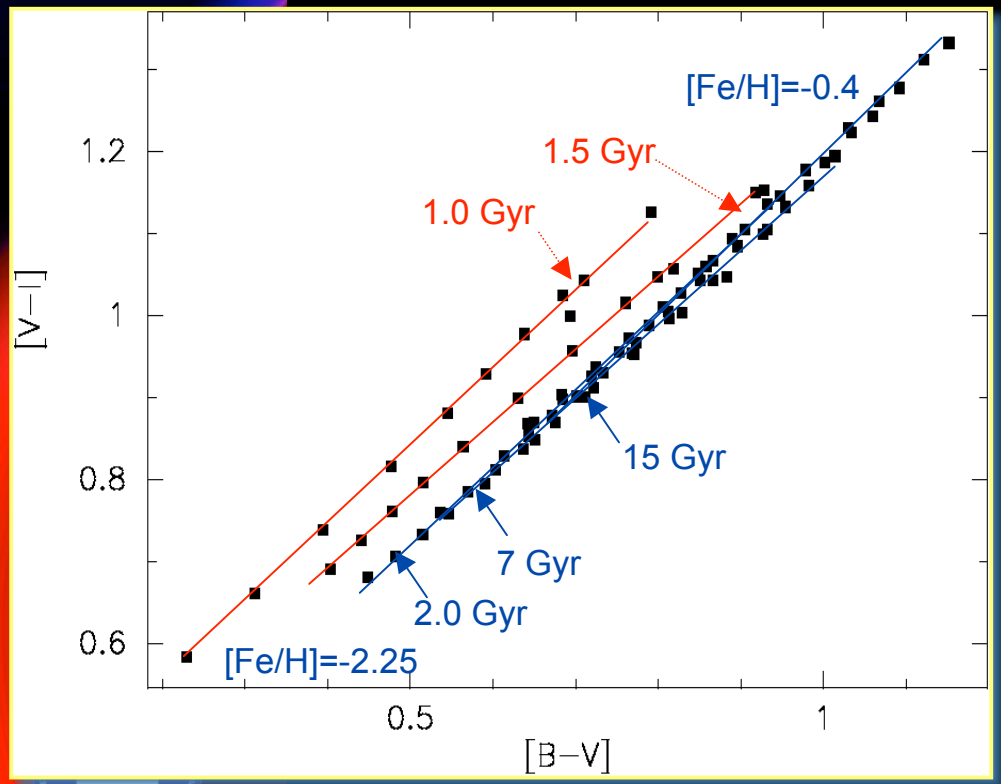

Models: Bruzual & Charlot (2003)

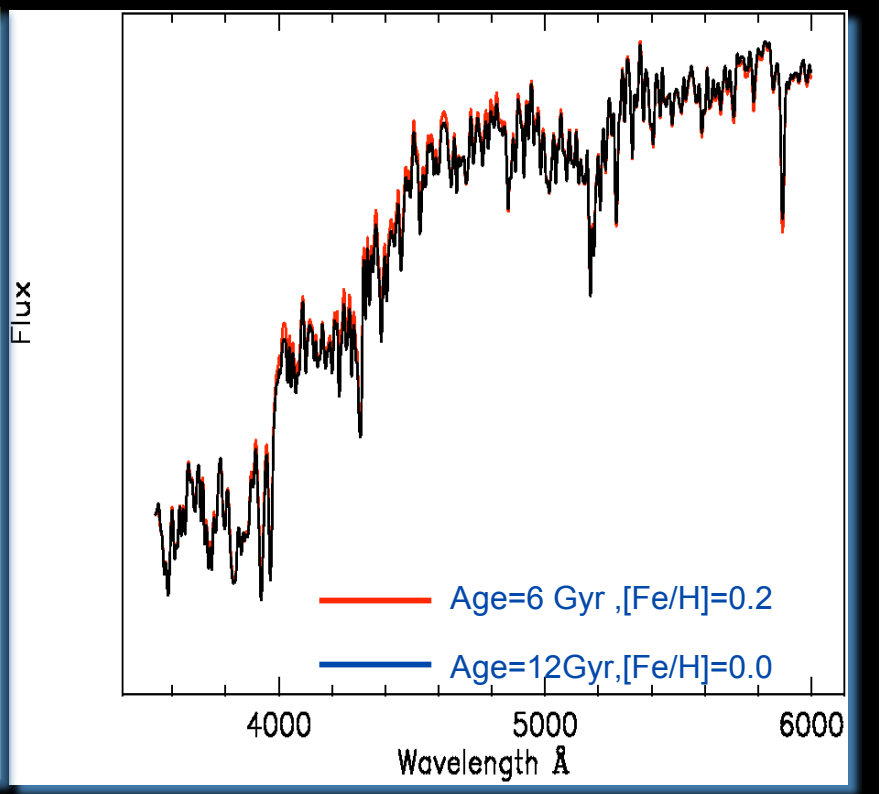

Models: Sanchez-Blazquez (Ph.D. thesis), Vazdekis et al. 2005 (in prep)

Some discrimination ...

Trager 2000

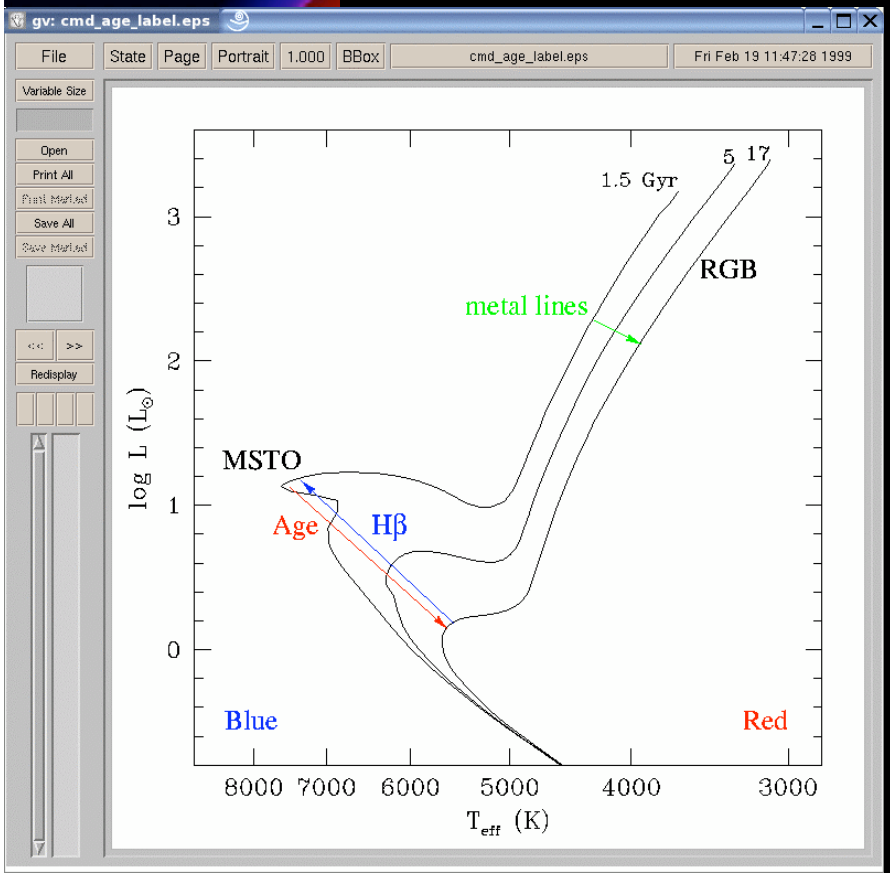

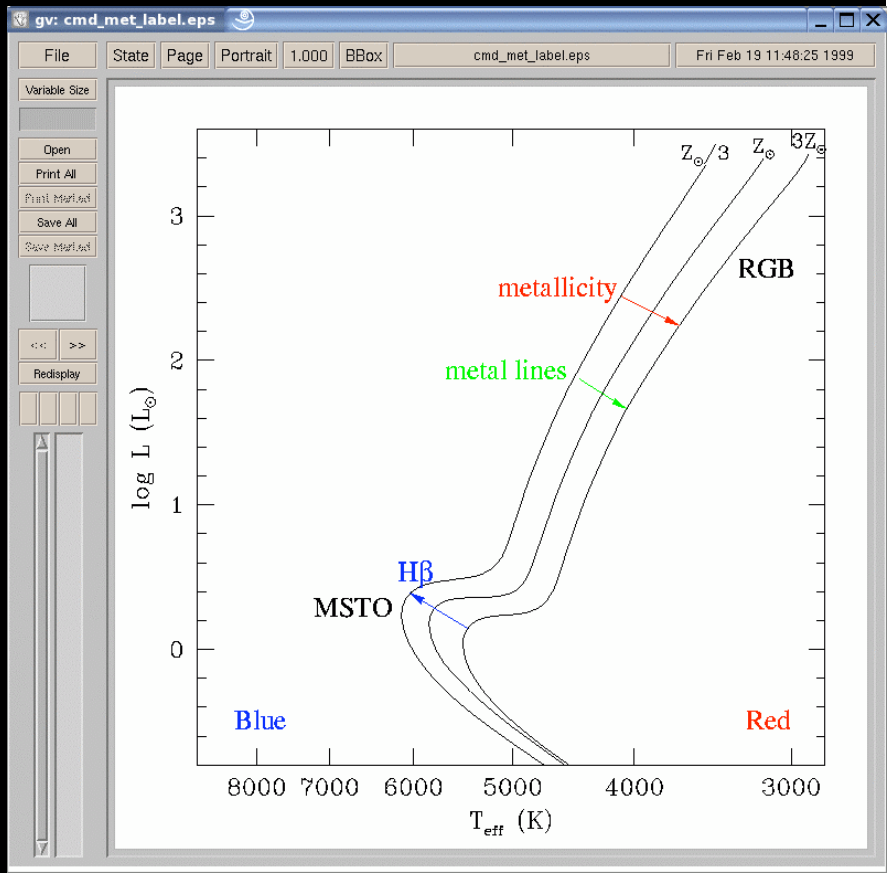

Stellar masses

Bell & de Jong 2001

- Flipside of age/met/dust degeneracy

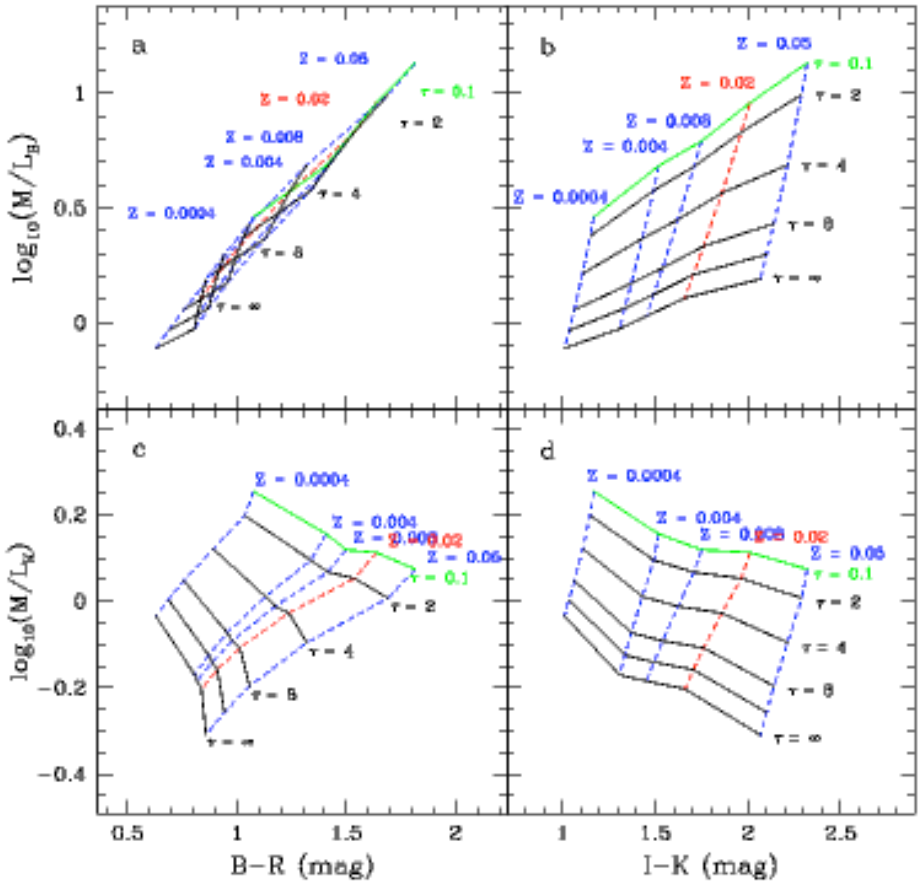

FIG. 2.— Trends in simple exponential SFH model stellar M/Ls with color. Stellar M/Ls for a Salpeter IMF in B (panels a and b) and K (panels c and d) of single metallicity exponentially declining star formation rate models from Bruzual & Charlot (2001) are shown against the model $B-R$ (panels a and c) and $I-K$ (panels b and d) broadband colors. Models of the same e-folding time scale τ have been connected by solid lines, models of the same metallicity Z are connected by dashed lines.

Heidelberg
March-April 2008

Effects of bursts

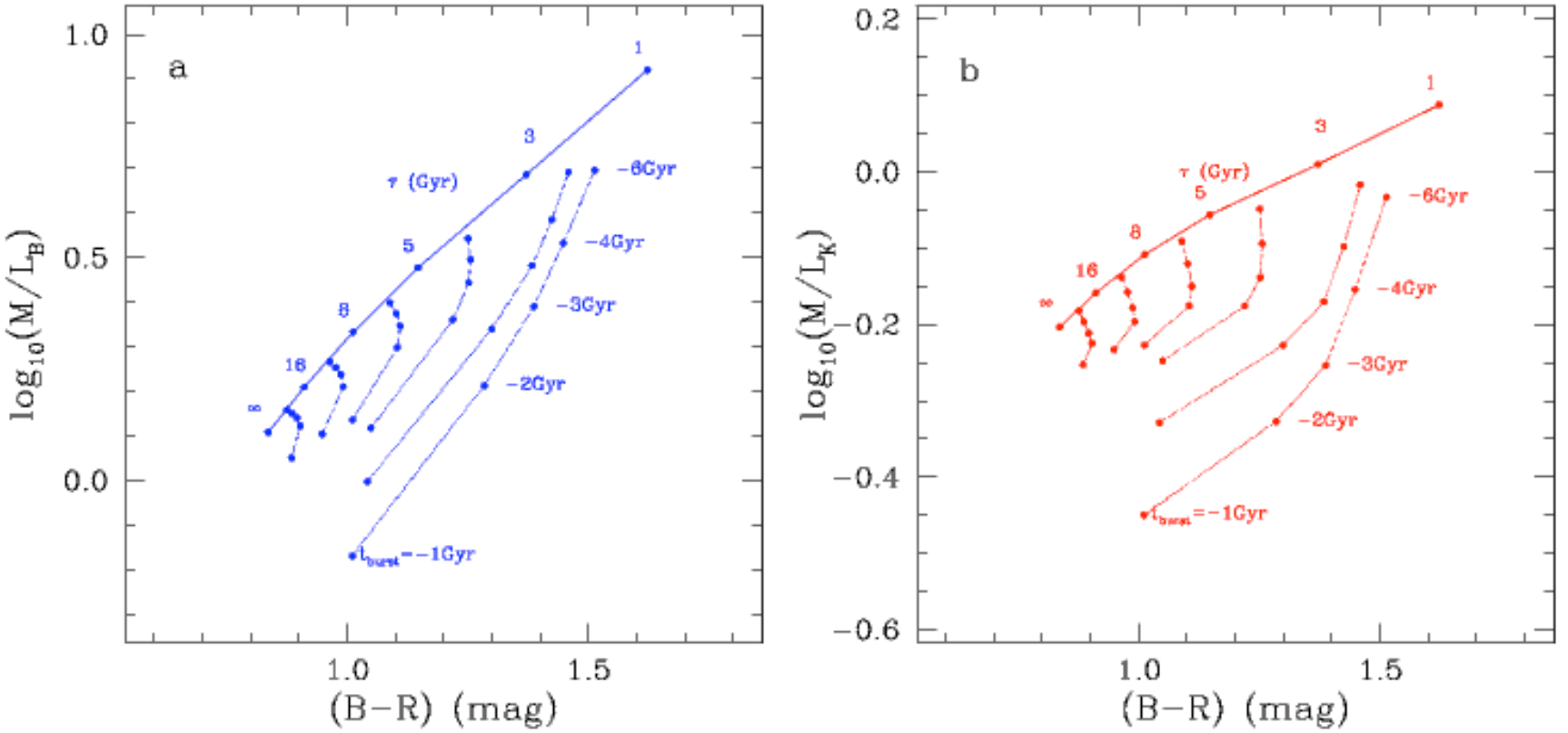

FIG. 5.— Color–M/L relations in B (a) and K (b) for a sequence of exponential declining star formation rate solar metallicity models of age 12 Gyr with 10% mass fraction added in 0.5 Gyr star bursts. The solid line connects the exponential SFH models with different e-folding times scales τ. The dotted lines connect models of the same τ value, but with added star bursts occuring 1, 2, 3, 4 or 6 Gyr ago.

Normalisation : stellar IMF

- Normalisation depends on stellar IMF
- Salpeter IMF
  - too much mass in low-mass stars
- Chabrier / Kroupa 2001 OK…

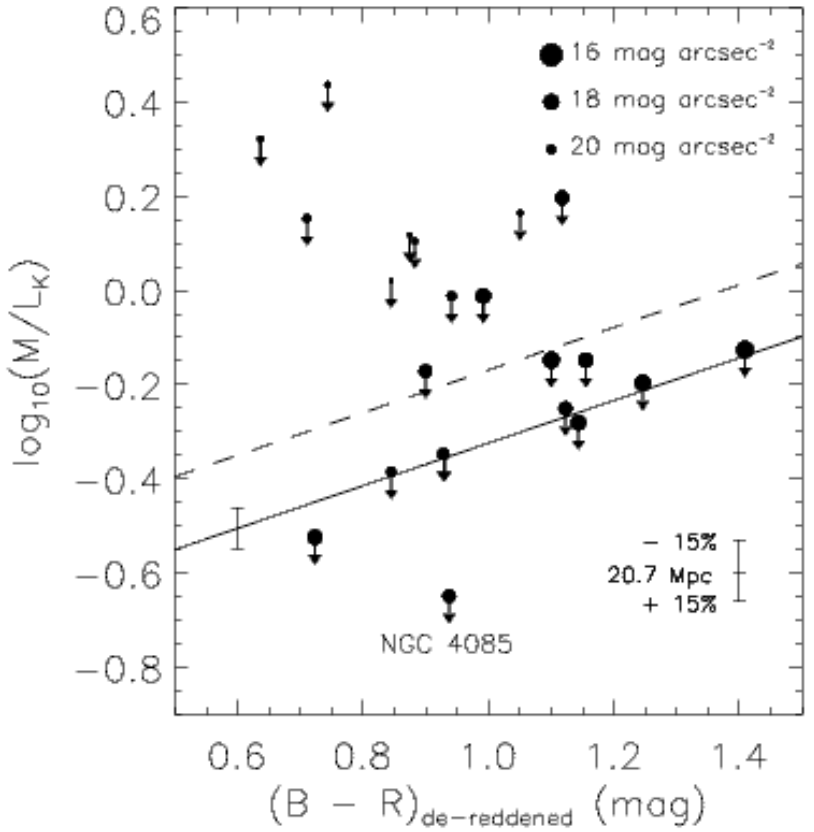

FIG. 6.— Observed K band maximum disk stellar M/Ls against de-reddened $B-R$ color. The data are from K band imaging and HI rotation curves from Verheijen (1997, Chapter 6), rescaled to a distance of 20.7 Mpc (Sakai et al. 2000): the effect on the maximum disk M/Ls of a $\pm 15\%$ Ursa Major Cluster distance error is also shown. Overplotted is the least-squares fit to the correlation between color and stellar M/L for the formation epoch with bursts model assuming a Salpeter (dashed line) and a scaled-down Salpeter IMF (solid line). We also show the RMS spread of the formation epoch with bursts model around the color–M/L relation on the solid line as an error bar. NGC 4085 is highlighted: it has a poorly resolved rotation curve, which biases the maximum disk M/L downwards. Symbol size is coded by inclination-corrected K band central surface brightness.

Heidelberg
March-April 2008

Stellar masses

- Assumption - universal IMF
- Methods
  - SED fitting Spectrum fitting
  - Comparison with dynamics: ~0.1 dex scatter

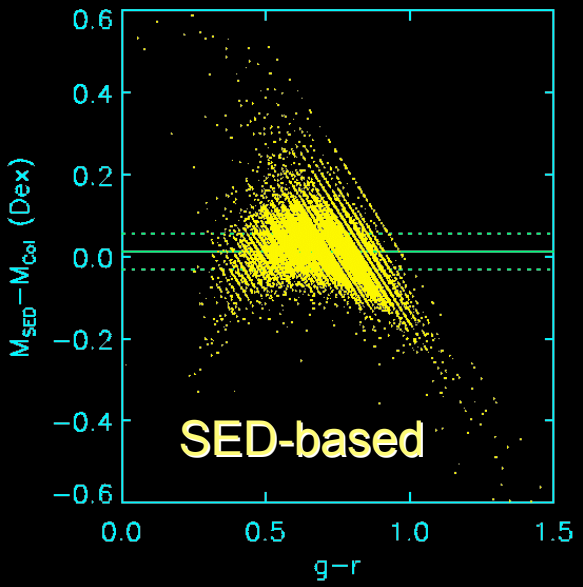

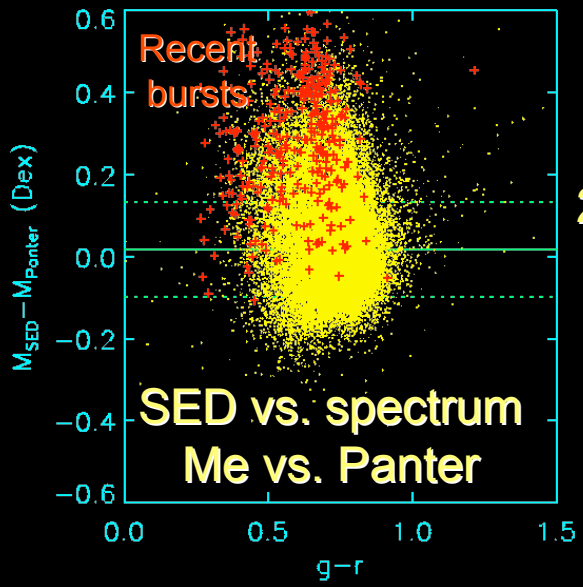

de Jong & Bell, 2002-2009; in prep.

Comparing M* for SDSS galaxies

Heidelberg
March-April 2008

Eric Bell

Example stellar M/L calibns

TABLE A7

STELLAR M/L RATIO AS A FUNCTION OF COLOR

Color	a_g	b_g	a_r	b_r	a_i	b_i	a_z	b_z	a_J	b_J	a_H	b_H	a_K	b_K
$u-g$	–0.221	0.485	–0.099	0.345	–0.053	0.268	–0.105	0.226	–0.128	0.169	–0.209	0.133	–0.260	0.123
$u-r$	–0.390	0.417	–0.223	0.299	–0.151	0.233	–0.178	0.192	–0.172	0.138	–0.237	0.104	–0.273	0.091
$u-i$	–0.375	0.359	–0.212	0.257	–0.144	0.201	–0.171	0.165	–0.169	0.119	–0.233	0.090	–0.267	0.077
$u-z$	–0.400	0.332	–0.232	0.239	–0.161	0.187	–0.179	0.151	–0.163	0.105	–0.205	0.071	–0.232	0.056
$g-r$	–0.499	1.519	–0.306	1.097	–0.222	0.864	–0.223	0.689	–0.172	0.444	–0.189	0.266	–0.209	0.197
$g-i$	–0.379	0.914	–0.220	0.661	–0.152	0.518	–0.175	0.421	–0.153	0.283	–0.186	0.179	–0.211	0.137
$g-z$	–0.367	0.698	–0.215	0.508	–0.153	0.402	–0.171	0.322	–0.097	0.175	–0.117	0.083	–0.138	0.047
$r-i$	–0.106	1.982	–0.022	1.431	0.006	1.114	–0.052	0.923	–0.079	0.650	–0.148	0.437	–0.186	0.349
$r-z$	–0.124	1.067	–0.041	0.780	–0.018	0.623	–0.041	0.463	–0.011	0.224	–0.059	0.076	–0.092	0.019
Color	a_B	b_B	a_V	b_V	a_R	b_R	a_I	b_I	a_J	b_J	a_H	b_H	a_K	b_K
$B-V$	–0.942	1.737	–0.628	1.305	–0.520	1.094	–0.399	0.824	–0.261	0.433	–0.209	0.210	–0.206	0.135
$B-R$	–0.976	1.111	–0.633	0.816	–0.523	0.683	–0.405	0.518	–0.289	0.297	–0.262	0.180	–0.264	0.138

Note. — Stellar M/L ratios are given by $\log_{10}(\mathrm{M/L}) = a_\lambda + (b_\lambda \times \mathrm{Color})$ where the M/L ratio is in solar units. If *all* galaxies are sub-maximal then the above zero points (a_λ) should be modified by subtracting an IMF dependent constant as follows: 0.15 dex for a Kennicutt or Kroupa IMF, and 0.4 dex for a Bottema IMF. Scatter in the above correlations is ~ 0.1 dex for all optical M/L ratios, and 0.1–0.2 dex for NIR M/L ratios (larger for galaxies with blue optical colors). SDSS filters are in AB magnitudes; Johnson BVR and JHK are in Vega magnitudes.

Kroupa / Chabrier -- actually -0.1 dex (Borch et al. 2006)

Heidelberg
March-April 2008

Eric Bell

Gas metallicities

Using OIII 4363 to get effective temperature,
electron density from OII,
then can solve for metallicity using strong lines

Strong line methods -
R23 = (OII + OIII)/Hbeta

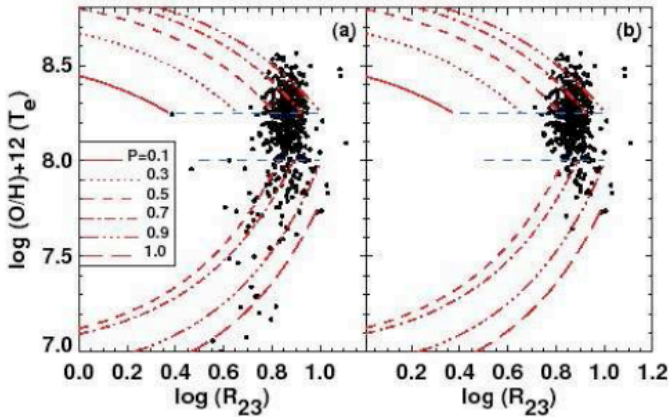

FIG. 11.— The observed relationship between the metallicities derived using the T_e method and the R_{23} line ratio for (a) all SDSS galaxies in our sample with measurable (S/N> 3) [O III] λ4363 fluxes, and (b) for the SDSS galaxies in our sample with measurable [O III] λ4363 lines that lie above the lowest 95 percentile line in the PP04 O3N2 calibration (Figure 10).

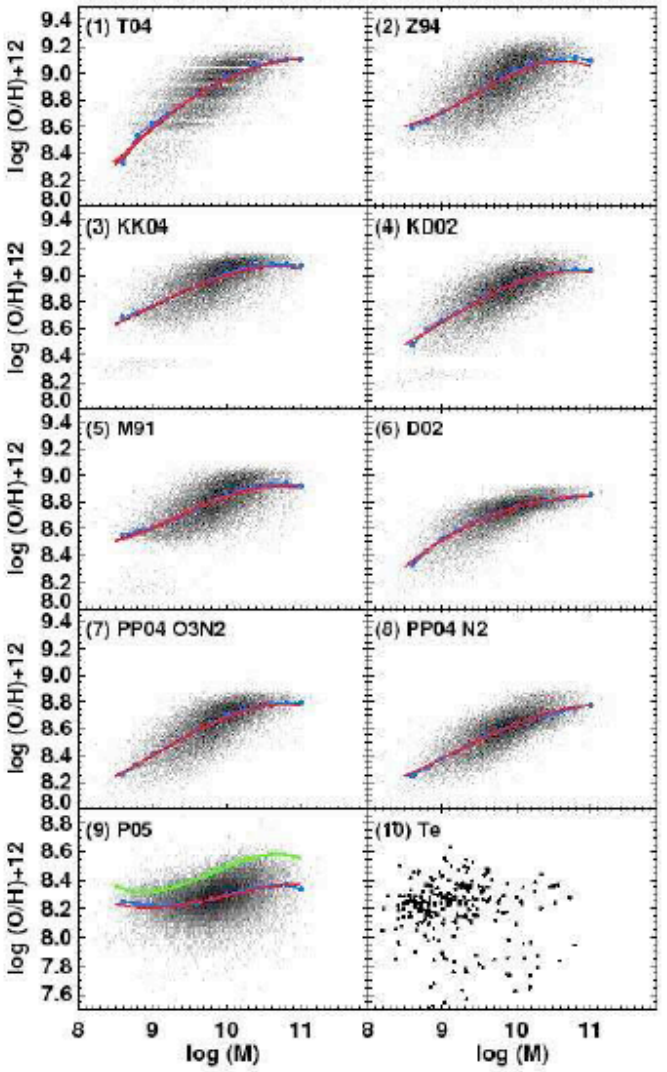

FIG. 1.— The mass-metallicity relation using the 10 different metallicity calibrations listed in Table 1. The red line shows the robust best-fitting 3rd-order polynomial to the data. The blue circles give the median metallicity within stellar mass bins of $\Delta \log(M/M_\odot) = 0.2$, centered at $\log(M/M_\odot) = 8.6, 8.8, ..., 11$. We use the updated calibration of P05 given by Pilyugin & Thuan (2005) in panel 9. The original P01 calibration is shown as a solid green line in panel 9.

Kewley & Ellison 2008

Electron temperature

Ratio of 4363
to 4959+5007
gives a measure
of electron temperature

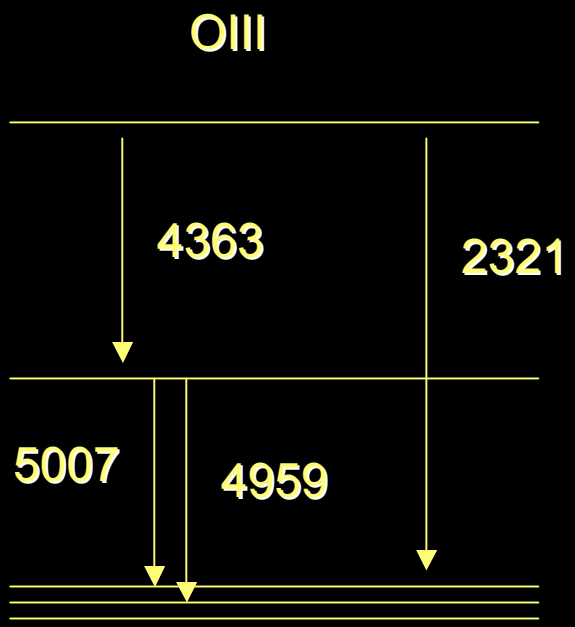

$$4959+5007 / 4363 = 7.73\, e^{33000/T} / (1 + 0.00045\, N_e/\mathrm{sqrt}(T))$$

Heidelberg
March-April 2008

Eric Bell

Gas conditions, continued

- Electron density (e.g., OII)…
  - Two levels with almost same energy difference but different angular momenta and different radiative transition probabilities.
  - At low N_e, every excitation has to de-excite with a photon, so transition probabilities don't matter
  - At high Ne, most de-excitations are from collisions, so transition probabilities matter very much indeed…

$$\frac{j_{\lambda 3729}}{j_{\lambda 3726}} = \frac{N_2 D_{5/2}}{N_2 D_{3/2}} \frac{A_{\lambda 3729}}{A_{\lambda 3726}} = \frac{3}{2} \frac{4.2 \times 10^{-5}}{1.8 \times 10^{-4}} = 0.35 \qquad (4.1)$$

Gas metallicities

Using OIII 4363 to get effective temperature,
electron density from OII,
then can solve for metallicity using strong lines

Strong line methods -
R23 = (OII + OIII)/Hbeta

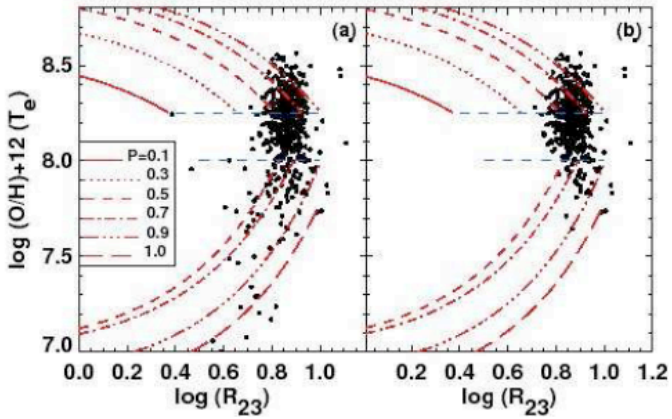

FIG. 11.— The observed relationship between the metallicities derived using the T_e method and the R_{23} line ratio for (a) all SDSS galaxies in our sample with measurable (S/N> 3) [O III] λ4363 fluxes, and (b) for the SDSS galaxies in our sample with measurable [O III] λ4363 lines that lie above the lowest 95 percentile line in the PP04 O3N2 calibration (Figure 10).

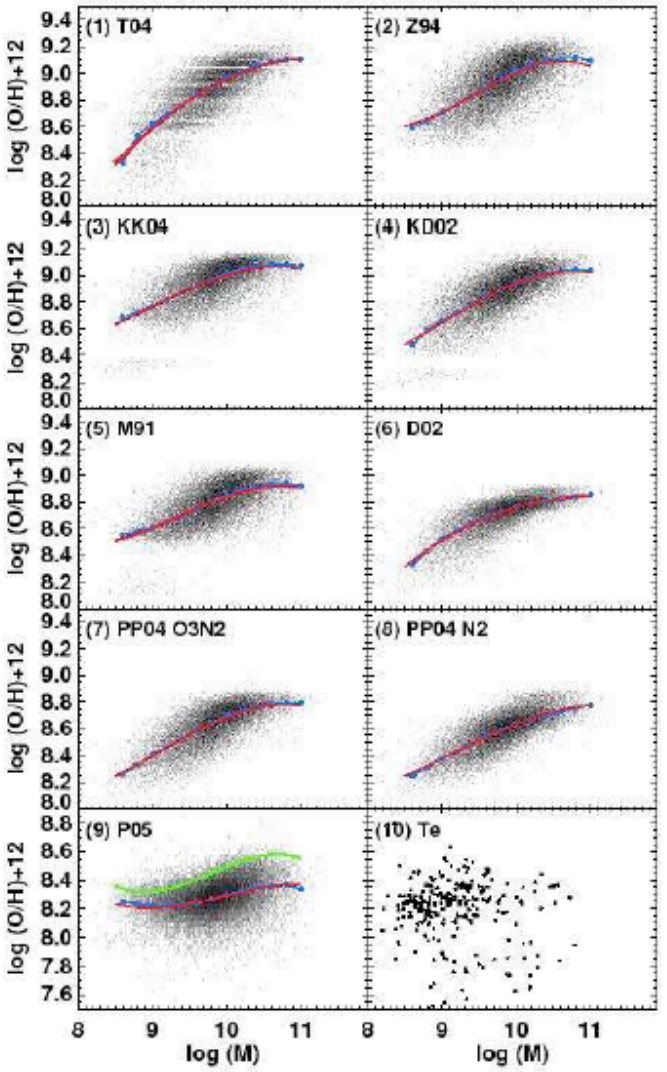

FIG. 1.— The mass-metallicity relation using the 10 different metallicity calibrations listed in Table 1. The red line shows the robust best-fitting 3rd-order polynomial to the data. The blue circles give the median metallicity within stellar mass bins of $\Delta \log(M/M_\odot) = 0.2$, centered at $\log(M/M_\odot) = 8.6, 8.8, ..., 11$. We use the updated calibration of P05 given by Pilyugin & Thuan (2005) in panel 9. The original P01 calibration is shown as a solid green line in panel 9.

Kewley & Ellison 2008

Star formation rates

- UV / reprocessed UV light (IR; can be heated through light from older stars)
- Measuring number of free electrons (ionising flux from v. hot stars)
  - Recombination lines Halpha, Pa alpha, etc.
  - Thermal radio flux
- Synchrotron (indirect; measures cosmic ray density and mag. field strength)

intercomparison

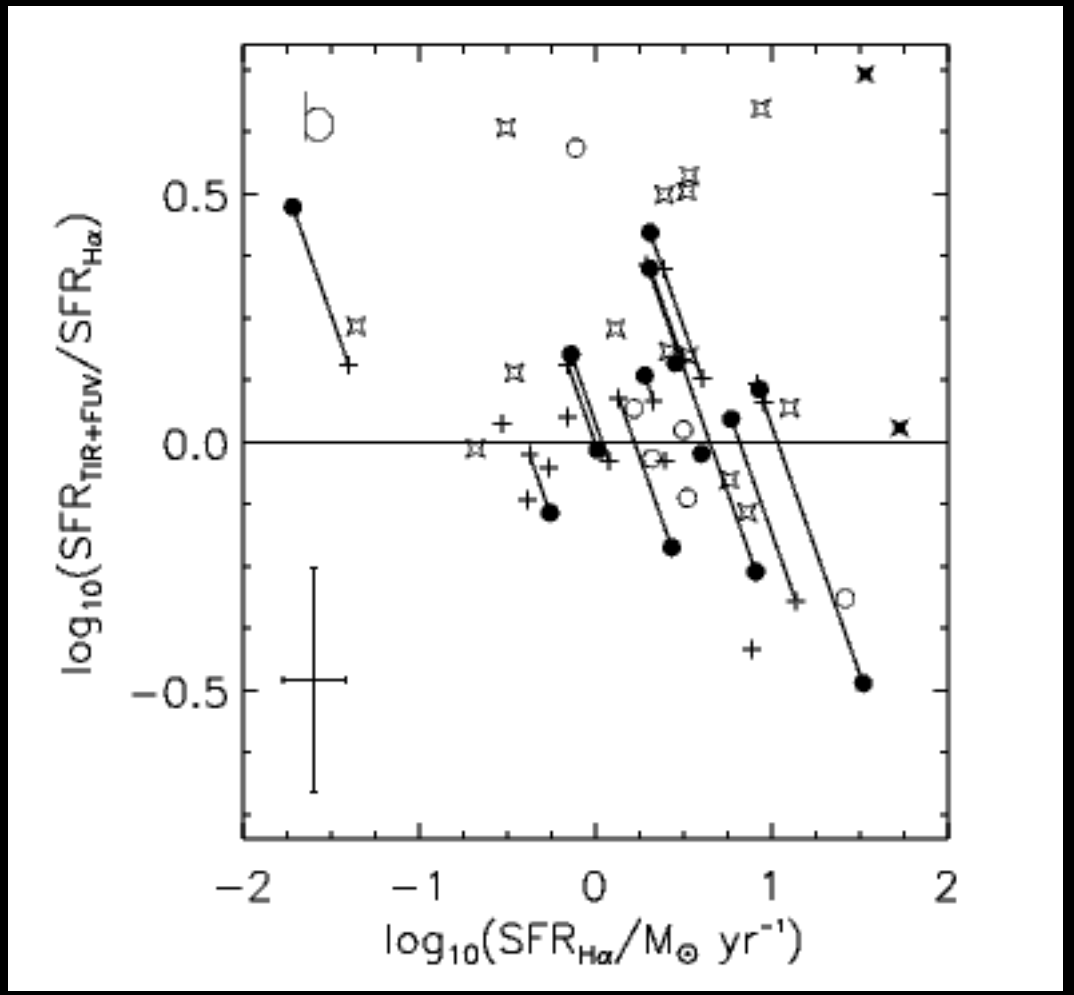

Heidelberg
March-April 2008

Eric Bell

Radio-FIR correlation

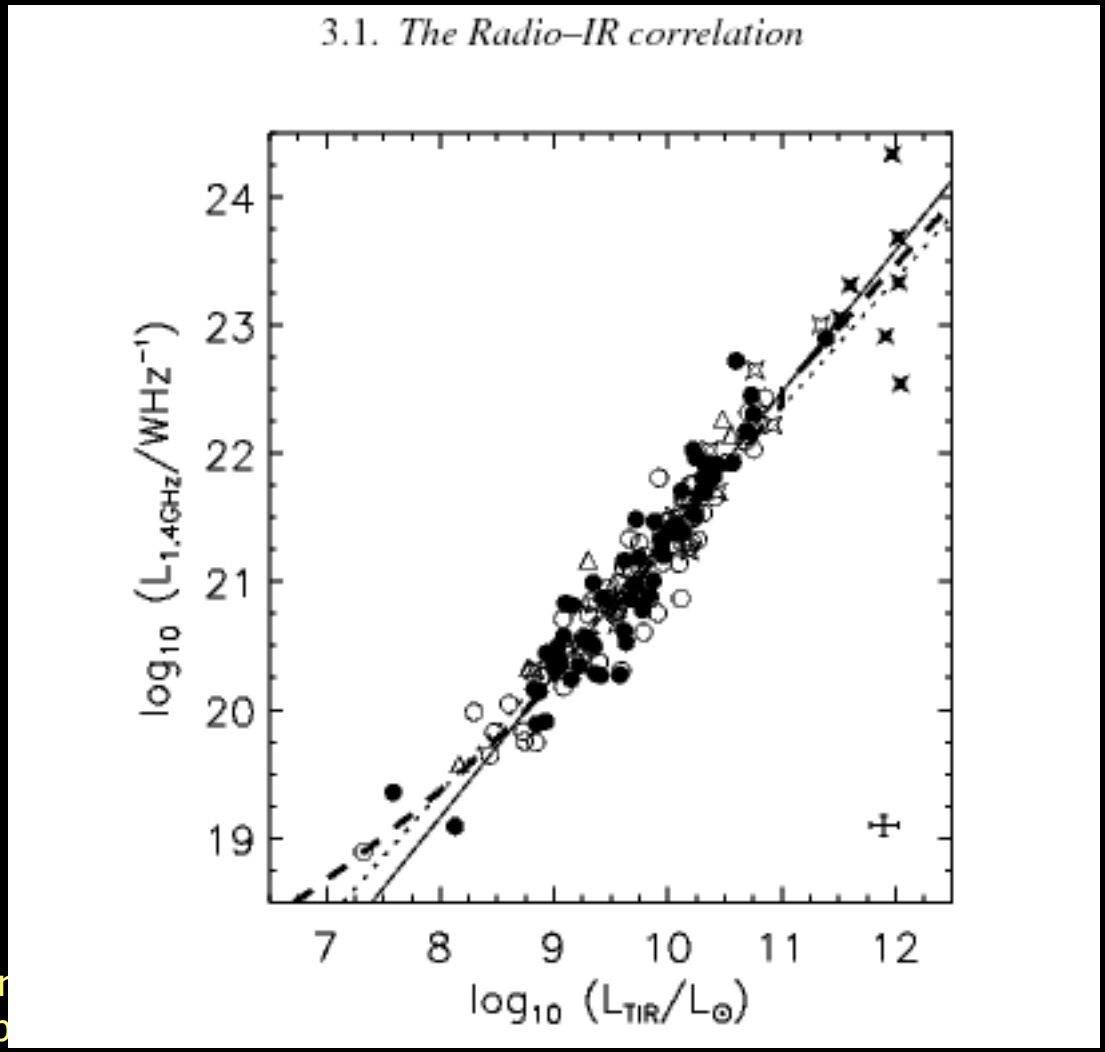

Simple toy model consideration

- Optical depth ∝ gas surface density * metallicity
  - Motivation - dust/gas ∝ metallicity
  - Total dust column ∝ gas column

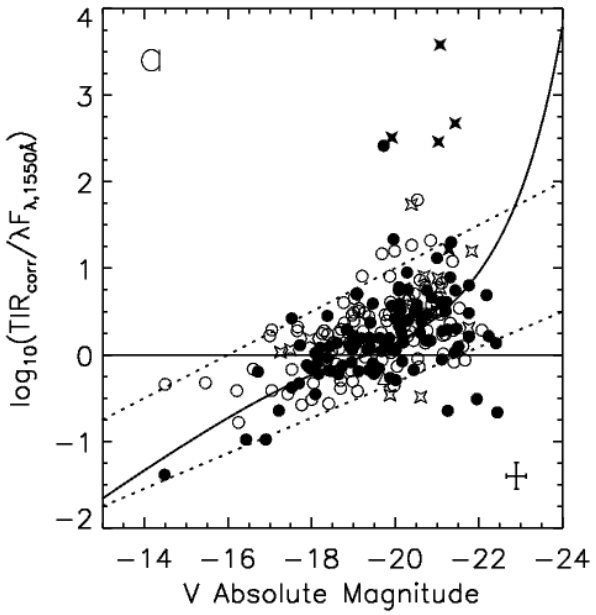

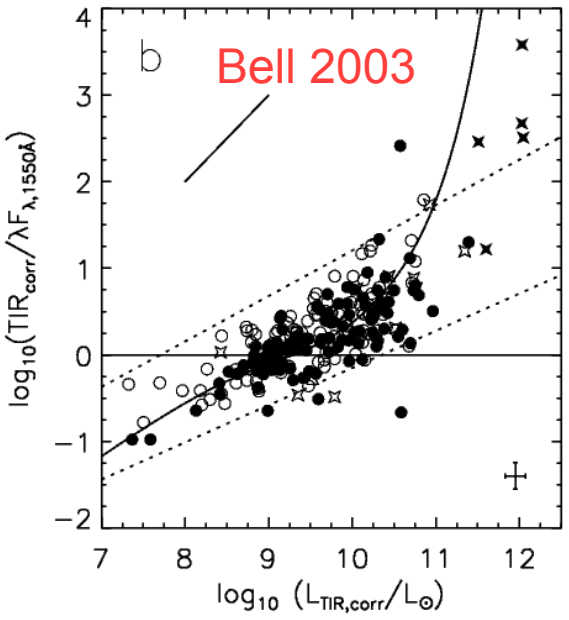

Eric Bell

Linear radio-FIR correlation: a conspiracy

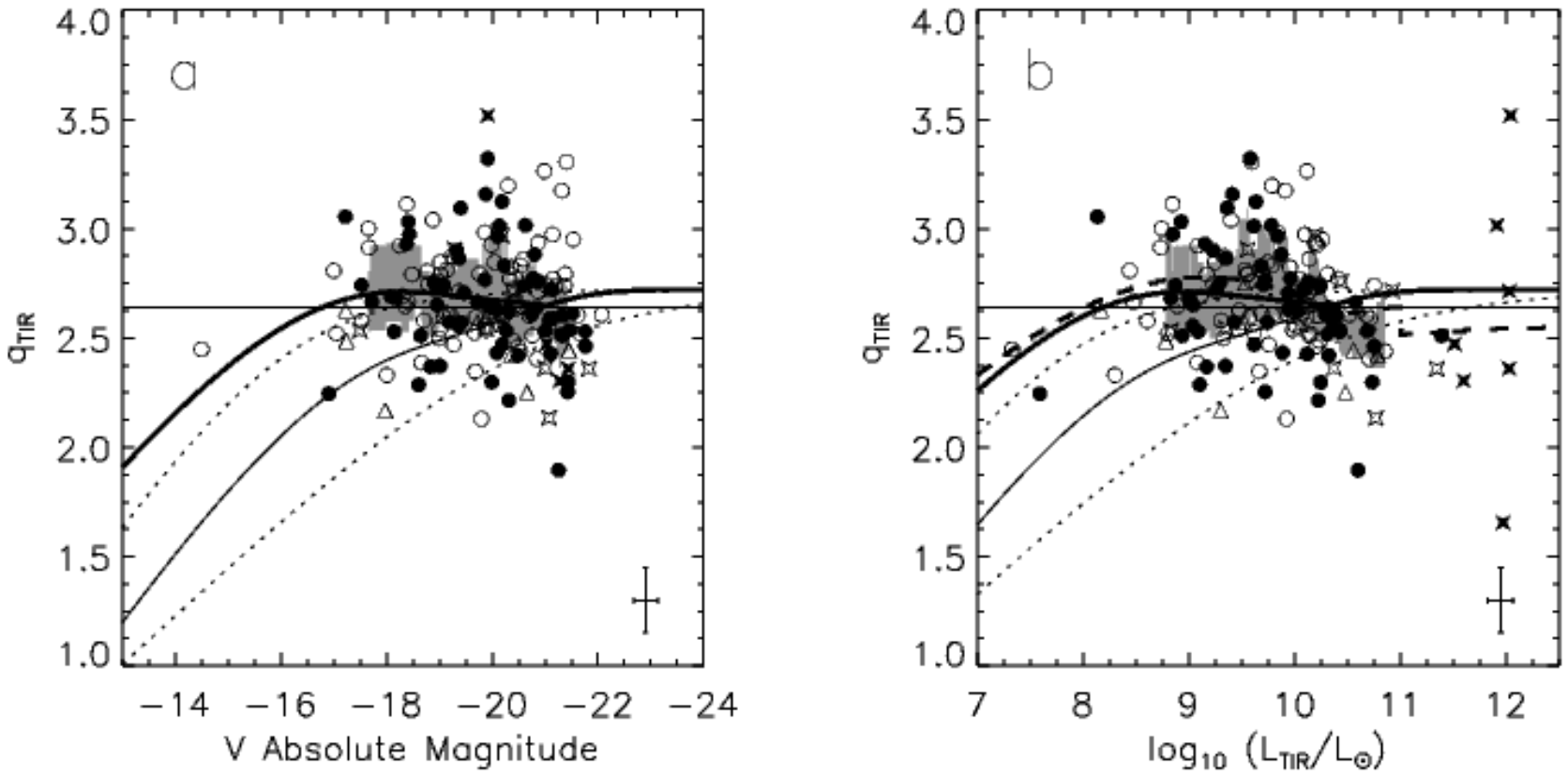

FIG. 4.— Trends in q_{TIR} with galaxy luminosity. Panel *a)* shows q_{TIR} against V-band absolute magnitude, and panel *b)* shows q_{TIR} against TIR luminosity. Symbols are the same as in Fig. 2. The shaded area shows the upper and lower quartiles as a function of luminosity: this shows, in a less noisy fashion, any trends between q_{TIR} and galaxy luminosity. The effect of trends in TIR/FUV with luminosity are plotted as thin dotted (the limits on TIR/FUV as a function of luminosity) and thin solid (the model TIR/FUV with luminosity) lines. If radio SFR were a perfect SF rate indicator, there should be a trend in q_{TIR} which follows the general trend of the thin dotted and solid lines. The thick solid line shows the final model presented in §5. The thick dashed line in panel *b)* shows the trend predicted by the final SF rate calibrations (see §6.1).

Calibrations; Kroupa 2001 or Chabrier 2003 IMF

- SFR ~ 9.8d-11 * (IR + 2.2UV) Bell+05
- SFR ~ 9.8d-11 * IR (1+sqrt[1d9/IR]) IR-only, Bell 03
- SFR_radio ~ pi d-22 * L_1.4GHz [L> Lc = 6.4d21 W/Hz]
- SFR_radio ~ pi d-22 * L_1.4GHz / (0.1+0.9*(L/Lc)^0.3) [L<Lc]
- SFR_Ha = 5.3d-42 L_Ha (ergs/s) Calzetti+07

Summary

- Stars / dust / gas shape the SED
  - Roughly 1/2 - 2/3 of all energy emitted by stars gets reprocessed by dust into the IR
- Can be translated into physical parameters if one makes assumptions
  - Stellar IMF
  - Star formation / chemical history
- Under these assumptions
  - Masses to 30%
  - SFRs to better than x2
  - Metallicities to x2
  - Ages hard; birthrates = SFR/(M^*/t_{hubble}) easier

Stuff to have added

- Steps in going from electron / star number (luminosity) to a *rate* of star formation

- Luminosity weighting.